

# Detection of krypton in xenon for dark matter applications

A. Dobi<sup>a</sup>, C. Davis<sup>a</sup>, C. Hall<sup>a</sup>, T. Langford<sup>a,b</sup>, S. Slutsky<sup>a</sup>, Y.-R. Yen<sup>a</sup>

<sup>a</sup>*Department of Physics, University of Maryland, College Park MD, 20742 USA*

<sup>b</sup>*Institute for Research in Electronics and Applied Physics, University of Maryland, College Park MD, 20742 USA*

---

## Abstract

We extend our technique for observing very small concentrations of impurities in xenon gas to the problem of krypton detection. We use a conventional mass spectrometer to identify the krypton content of the xenon, but we improve the sensitivity of the device by more than five orders of magnitude with a liquid nitrogen cold trap. We find that the absolute krypton concentration in the xenon can be inferred from the mass spectrometry measurements, and we identify krypton signals at concentrations as low as  $0.5 \times 10^{-12}$  mol/mol (Kr/Xe). This technique simplifies the monitoring of krypton backgrounds for WIMP dark matter searches in liquid xenon.

*Key words:*

xenon, krypton, cold trap, mass spectrometry, dark matter

---

## 1. Introduction

One of the primary challenges faced by liquid xenon WIMP dark matter experiments is the presence of trace amounts of radioactive krypton. Xenon itself has no long-lived radioactive isotopes which might act as background sources, but krypton includes the troublesome anthropogenic isotope  $^{85}\text{Kr}$ , a beta emitter with a Q value of 687 keV and a half-life of 10.76 years.  $^{85}\text{Kr}$  is created in nuclear power plants and released into the earth's atmosphere during fuel reprocessing, and its isotopic fraction at present is about  $2 \times 10^{-11}$  mol/mol ( $^{85}\text{Kr}/^{nat}\text{Kr}$ )[1]. Xenon, on the other hand, is extracted from the atmosphere with a residual krypton concentration typically ranging

from  $10^{-9}$  to  $10^{-6}$  mol/mol ( $^{nat}\text{Kr}/\text{Xe}$ ). Although this implies that the absolute concentration of  $^{85}\text{Kr}$  in xenon is rather small, the  $^{85}\text{Kr}$  beta decay is nevertheless highly problematic for dark matter experiments because these decays are not suppressed by self-shielding and because krypton cannot be separated from xenon with conventional chemical purifiers.

The acceptable krypton concentration for a particular experiment is determined by its design sensitivity and by its nuclear recoil discrimination factor. As an example, the LUX dark matter experiment, a dual phase liquid xenon TPC with a recoil discrimination factor of 99.5%, requires that the residual krypton concentration of the xenon target material be no more than  $\sim 3 \times 10^{-12}$  mol/mol ( $^{nat}\text{Kr}/\text{Xe}$ )<sup>1</sup>[2, 3] in order to be sensitive to a 100 GeV WIMP with a cross section as small as  $7 \times 10^{-46}$  cm<sup>2</sup>. Other liquid xenon detectors, such as XMASS[4], and XENON100[5, 6], also have demanding krypton goals, and future upgrades of these experiments will require reducing the krypton concentration even further.

To achieve these ultra-low krypton concentrations, commercially procured xenon must undergo additional processing via distillation or gas chromatography. Once this processing is complete, the residual krypton content of the xenon can be determined by low background counting of the  $^{85}\text{Kr}$  beta decays[7, 5], by chromatography[8], or by atmospheric pressure ionization mass spectroscopy (API-MS)[7]<sup>2</sup>. These methods have achieved a sensitivity of about  $\sim 10^{-12}$  mol/mol. Krypton monitoring is useful because it can confirm that the processing has been successful prior to full detector operations, and because it can constrain the background count rate due to  $^{85}\text{Kr}$  in the WIMP search data.

In this article we show that very small krypton concentrations can be observed in xenon gas using a mass spectrometry technique which we previously developed to detect electronegative impurities in xenon[10]. The method is inexpensive, highly sensitive, and it could be quickly adopted and applied by many working dark matter experiments.

---

<sup>1</sup>All concentrations in this article refer to the natural krypton to xenon ratio, measured in units of mol/mol, unless otherwise indicated.

<sup>2</sup>It has also been suggested that atomic trap trace analysis may be sensitive to krypton at the level of  $3 \times 10^{-14}$  mol/mol, but this method has not yet been demonstrated for this application[9].

## 2. Xenon cold trap mass spectrometry

We use a residual gas analyzer (RGA) mass spectrometer to analyze our xenon by introducing a small quantity of the gas into the RGA's vacuum enclosure through a leak valve. Since the partial pressure of each component species is proportional to both its absolute concentration and to the flow rate through the analysis system, by controlling for the flow rate the partial pressures can be interpreted in terms of the absolute concentrations. The measurement is calibrated by preparing samples of xenon gas with known impurity concentrations for the various species of interest by directly mixing known quantities of impurities with a known amount of xenon. The flow rate can be controlled either by measuring the actual flow rate in real time or by using a standard leak-valve setting whose flow rate was previously calibrated.

Since the partial pressures of all species are proportional to the flow rate, the RGA signals can be vastly increased simply by opening the leak valve further. However, the RGA cannot be operated above some maximum total pressure, typically about  $10^{-5}$  Torr, and the total pressure is dominated by the xenon present in the gas sample. This limits the maximum flow rate that can be used. For example, if krypton can be detected by the RGA at a partial pressure of  $\sim 10^{-12}$  Torr, and the xenon pressure is  $10^{-5}$  Torr, then the limit of detection is about one part in  $10^7$ . Since we are interested in krypton concentrations at the level of  $10^{-12}$  mol/mol, this is inadequate for our purposes.

We solve the saturation problem simply by removing most of the xenon from the gas sample with a liquid nitrogen cold trap placed between the leak valve and the RGA which allows the flow rate to be vastly increased without saturating the RGA. For the bulk xenon, the pressure is adequate for xenon ice to form ( $>1.8$  mTorr at 77 K) [11]. So the xenon pressure is held fixed at its vapor pressure. For many common species however, the partial pressure is below the solid-vapor or liquid-vapor equilibrium. This prevents the impurities from becoming trapped. In our previous paper, we showed that impurity species such as oxygen, nitrogen, and methane pass through the cold trap in large quantities, and that their partial pressures, corrected for flow rate, remain proportional to their absolute concentrations. The sensitivity to oxygen, nitrogen, and methane was found to be  $0.66 \times 10^{-9}$ ,  $9.4 \times 10^{-9}$ , and  $0.49 \times 10^{-9}$  (mol/mol), respectively [10].

Here we extend the technique to observe krypton in xenon. We expect that krypton could be observed in very small quantities by the RGA because

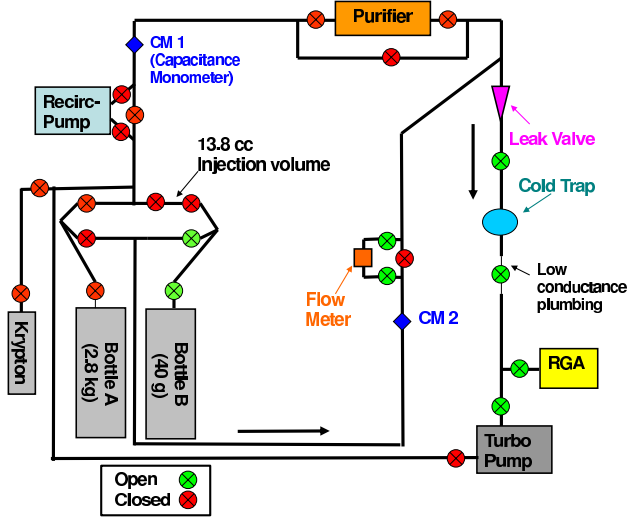


Figure 1: Diagram of the xenon handling system. The flow pattern shown is typical of a measurement described in section 5.

there are very few background species which could obscure the krypton signal. In fact, we find that we are able to detect krypton in xenon at a concentration of  $0.5 \times 10^{-12}$  mol/mol, which makes this technique better than or comparable to existing methods, and sensitive enough to be useful for working dark matter experiments.

### 3. Apparatus and procedures

A diagram of our analysis apparatus and our xenon handling system is shown in Figure 1 and Figure 2. The xenon of interest is admitted into the analysis system through an ultra-high vacuum leak valve (Kurt Lesker part number VZLVM940R). It passes through a liquid nitrogen cold trap and a section of low-conductance plumbing before reaching an SRS RGA200 mass spectrometer. The low-conductance plumbing is necessary to reduce the xenon partial pressure from  $1.8 \times 10^{-3}$  Torr (its vapor pressure at liquid nitrogen temperature) to  $< 10^{-5}$  Torr. This ensures that the RGA, with the electron multiplier on, remains unsaturated. We use a fully open hand valve for the low-conductance element.

The cold trap is constructed from 1.5" OD stainless-steel tubing, welded

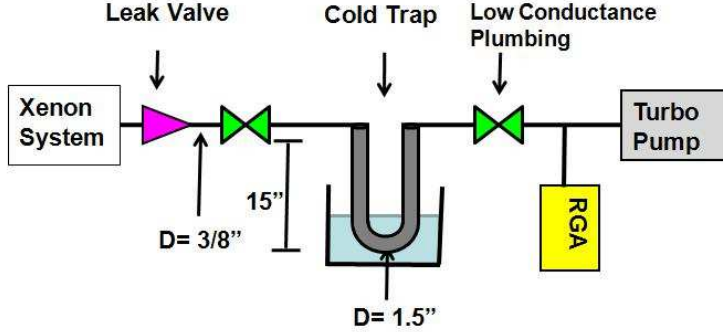


Figure 2: Diagram of the cold trap mass spectrometer analysis system.

into a U shape with a radius of 2.5" and 12.5" linear inlet and outlet legs<sup>3</sup>. The tubing diameter is chosen to allow a significant amount of xenon to be analyzed before the growth of xenon ice blocks the flow of gas through the analysis system. We find that the liquid nitrogen level must be high enough to submerge the bottom of the cold trap U, but otherwise its level is not critical.

We use several procedures to calibrate and monitor the flow rate through the leak valve. First, we calibrate the flow rate directly for a variety of leak valve settings using a fixed volume of xenon gas ( $\sim 1$  liter) at the leak valve input. We measure the pressure drop in this volume with a capacitive manometer (Type 627D Baratron) as the gas flows through the leak valve to infer the flow rate for each leak valve setting. We find that the flow rate is repeatable to within 10% simply by returning the leak valve to the same indicator marking on its dial. Second, we also measure the flow rate directly using a MKS model 179A mass flow meter which has been calibrated for use with xenon gas. Third, when the xenon under analysis contains a small, constant concentration of a tracer gas which is unaffected by the cold trap, such as argon or helium, then the partial pressure of the tracer can be used to accurately monitor the leak rate in real time with the RGA itself. This eliminates the systematic error due to the leak valve dial setting and RGA gain drift. We use this method in Section 4.

To calibrate the partial pressure measurements of the RGA in terms of

---

<sup>3</sup>We have also constructed working cold traps from standard vacuum plumbing components with 2.75" CF flanges.

the true krypton concentration, we insert known quantities of krypton into the xenon using a krypton gas cylinder (99.999% krypton purity). The injection volume is  $13.8 \pm 0.1$  cc of plumbing monitored by a pressure gauge, accurate within 0.1 Torr, and isolated by two valves. We inject krypton with pressures above 20 Torr, and further reduce the pressure by volume sharing. The krypton is combined with the xenon by flowing the xenon through the injection volume and collecting the gases in a recovery bottle where they mix.

To perform a measurement, first we submerge the cold trap in liquid nitrogen while it is pumped to ultra-high vacuum by the turbo-molecular pump, typically reaching a vacuum of  $4 \times 10^{-8}$  Torr. We then open the leak valve in two steps. In the first step, we use a very small leak rate, less than  $10^{-4}$  standard liters per minute (SLPM), which allows xenon ice to form in the cold trap, establishes the fixed xenon partial pressure, and flushes some trace background gases out of the analysis system plumbing. We wait for several minutes for the partial pressures of all species to stabilize, and then we open the leak valve to the desired flow rate for purity analysis. In general, the best sensitivity is obtained by using the maximum possible flow rate. In some cases the flow rate is limited by the partial pressure of non-xenon impurity species such as oxygen, nitrogen, or argon. Since these species are not removed by the cold trap, their presence in the xenon gas will eventually cause the RGA to saturate as the flow rate is increased. For the very best sensitivity, the xenon should be free from extraneous impurity species.

#### 4. Response of the analysis system to krypton

In our first series of experiments, we confirm that the krypton partial pressure observed by the RGA is indeed linear in the true concentration by injecting known amounts of krypton into our 2.8 kg xenon supply. For these measurements, the xenon supply bottle continuously feeds xenon into the system through a regulator, maintaining a constant pressure at the leak valve input. This insures that the leak rate into the analysis system is nearly constant throughout the measurement, which simplifies the data analysis.

To precisely monitor the leak valve flow rate in real time, we use argon as a tracer gas. Our 2.8 kg xenon supply contains an argon concentration of about  $10^{-6}$  mol/mol, and since the argon level is constant from one injection experiment to the next (because the injected gas is 99.999% krypton, with only trace quantities of argon), the argon partial pressure serves as a convenient proxy for the gas flow rate through the analysis system. Under these

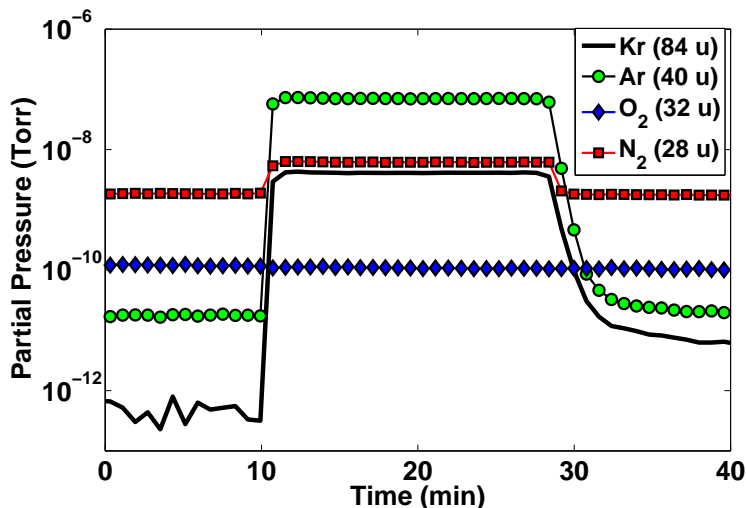


Figure 3: The results for a typical purity measurement with constant flow rates. At  $t = 10$  minutes the leak valve is opened and a measurement is made with a flow rate of 0.10 SLPM. This sample of xenon contained  $40 \times 10^{-9}$  mol/mol nitrogen,  $4 \times 10^{-6}$  mol/mol argon, and  $66.4 \times 10^{-9}$  mol/mol krypton. At  $t = 28$  minutes the leak valve is closed.

conditions, the leak valve can be opened to an arbitrary setting, and the krypton-to-argon partial pressure ratio should be proportional to the true krypton concentration.

A typical measurement is shown in Figure 3. At  $t = 0$ , xenon ice has already been established in the cold trap and backgrounds have stabilized, and the measurement begins at  $t = 10$  minutes, with a flowrate of 0.10 SLPM. Krypton, argon, and nitrogen are clearly present in the sampled gas, while the oxygen concentration is less than  $0.7 \times 10^{-9}$  mol/mol. At  $t = 28$  minutes the leak valve is closed.

In Figure 4 and Table 1 we show the krypton-to-argon partial pressure ratio as a function of the amount of krypton which we inject into our xenon supply. The partial pressure recorded by the RGA is averaged during the measurement yielding a statistical uncertainty of less than 1%. The uncertainty in the krypton to xenon ratio after an injection is 1%, from the uncertainty in the xenon mass ( $2800 \pm 20$ g), the injection volume, and the error on the pressure gauge. As shown in Table 1 each gas sample was measured at least twice to study the repeatability of the krypton-to-argon ratio for a fixed purity concentration. We find the ratio repeatable to about 1%.

$\Delta\rho(\text{Kr})$ ( $10^{-9}$ mol/mol)	$P_{\text{Kr}}$ (84 u) ( $10^{-9}$ Torr)	$P_{\text{Ar}}$ (40 u) ( $10^{-9}$ Torr)	$P_{\text{Kr}}/P_{\text{Ar}}$ (Torr/Torr)
0	4.11	70.3	0.0584
7.37	5.90	91.2	0.0647
	6.02	91.9	0.0655
18.4	7.00	93.7	0.0747
	6.60	87.8	0.0752
33.1	7.88	89.6	0.0879
	7.51	86.0	0.0873
	8.05	92.0	0.0876
	7.76	89.1	0.0871

Table 1: Krypton and argon partial pressures as a function of the injected krypton concentration ( $\Delta\rho(\text{Kr})$ ). Each gas sample was measured at least twice to confirm the repeatability of the Kr-to-Ar ratio. The uncertainty is the amount of krypton injected depends on the error in the injection volume and the error in the pressure gauge, combined they are less than 1%. The partial pressure recorded by the RGA is averaged during the measurement yielding a statistical uncertainty of 1% in partial pressure.

The absolute concentration of the argon is known only to within 50% ( $1 \pm 0.5$  ppm), however, the absolute concentration is not relevant, since we only use the argon as a flow rate standard.

The krypton-to-argon ratio is found to be linear in the injected concentration, which confirms that the cold trap allows the krypton to pass through as desired. Additional data confirms that it is also linear in the flow rate as observed for other species [10]. In total we injected  $33.1 \times 10^{-9}$  mol/mol of krypton, which resulted in a total increase in the krypton-to-argon ratio of a factor of 1.50 relative to the vendor-supplied xenon. From this we infer that the krypton concentration was  $(66.4 \pm 4) \times 10^{-9}$  mol/mol before our injections, and  $(99.5 \pm 4) \times 10^{-9}$  mol/mol after injections.

## 5. Detection of krypton at the $10^{-12}$ mol/mol level

The measurements described in Section 4 allow us to quantify the response of the analysis system to krypton. For example, the data in Table 1 shows a krypton partial pressure of  $7.9 \times 10^{-9}$  Torr, for a flow rate of 0.1 SLPM, and a krypton concentration of  $99.5 \times 10^{-9}$  mol/mol. Therefore, the analysis system response to krypton is 0.79 Torr/(SLPM  $\cdot$  mol/mol). Since the fluctuations in the RGA reading at 84 AMU (Atomic Mass Unit)



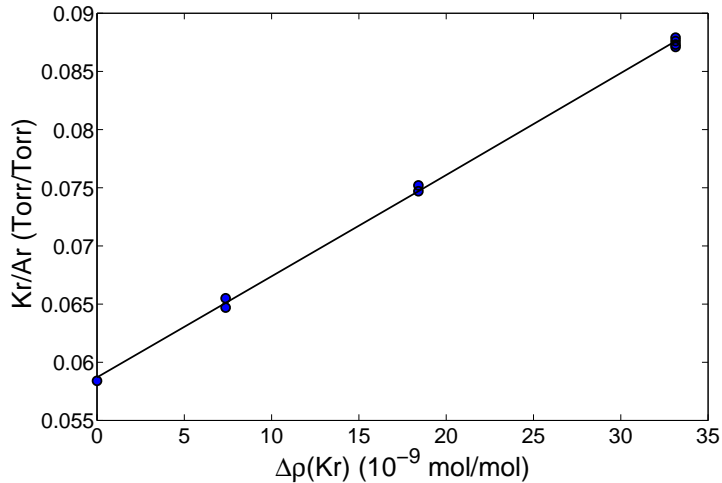


Figure 4: Krypton-to-argon partial pressure ratio versus the injected krypton concentration ( $\Delta\rho(\text{Kr})$ ). Repeated measurements are shown as separate data points. The non-zero y-intercept value is due to the krypton present in our vendor supplied xenon before our injections. Each gas sample was measured at least twice to gauge the systematic uncertainty in the RGA’s partial pressure measurements for a fixed concentration of krypton. We infer an uncertainty of 1% in the krypton-to-argon partial pressure ratio for a fixed concentration of krypton. Error bars are not plotted as they are too small to be seen on the graph

are  $\sim 3 \times 10^{-13}$  Torr, we expect that a concentration of  $1 \times 10^{-12}$  mol/mol krypton could be detectable at a flow rate of  $\sim 0.4$  SLPM. However, as shown in Figure 3, our xenon supply contains significant argon and nitrogen. Since these trace gases are not removed by the cold trap, they will cause the RGA to saturate at flow rates above 0.1 SLPM, with the argon being the leading problem. This would limit our krypton sensitivity to about  $4 \times 10^{-12}$  mol/mol. To detect krypton at lower concentrations it is necessary to remove these trace impurities.

Nitrogen can be removed from xenon using standard getters [12], but argon cannot. We first tried to remove the argon by freezing the xenon in its supply bottle with liquid nitrogen and pumping on the vapor with the turbo-molecular pump. This strategy proved to be inefficient, probably because the argon is trapped in the xenon ice requiring long diffusion times to escape. However, we successfully purified a small quantity of xenon using the cold trap itself. We allowed approximately seven standard liters of xenon to slowly leak into the cold trap while continuously pumping with a turbo-pump. We

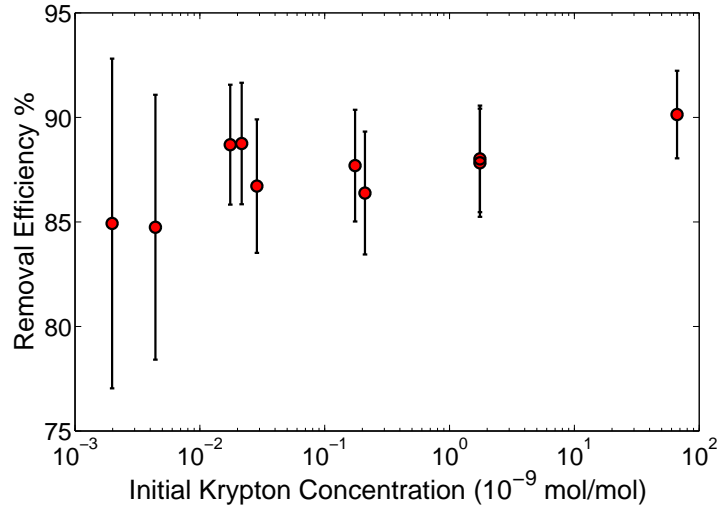


Figure 5: One pass krypton removal efficiency of the coldtrap vs. initial concentration, for several purification cycles.

repeated this process several times and during each cycle we measured the remaining krypton concentration with the RGA. We found that the krypton and argon levels were significantly reduced after each pass. We guess that the reduction comes about because the turbo pump is able to remove the krypton and argon before they become permanently trapped in the slowly forming xenon ice.

The average argon and krypton one-pass purification efficiencies were determined to be 99.4% and 87% respectively. We find that the krypton purification efficiency remains roughly constant vs. initial concentration over five orders of magnitude, shown in Figure 5. The removal efficiencies are derived assuming that the RGA's response to krypton is linear in concentration, which was later confirmed (see Figure 7). The uncertainty in the purification efficiency is derived from the maximum deviation from the linear response reported in Table 2. We do not include the argon removal efficiency in Figure 5 because we only have one measurement for argon. After the second pass, argon was not detectable by the RGA due to interference from doubly ionized krypton. This procedure ultimately produced a 40 gram sample of xenon with much less than  $1 \times 10^{-12}$  mol/mol argon and krypton.

Starting with this 40 gram sample of de-argonated and de-kryptonated xenon gas, we created xenon with known krypton concentration by mixing

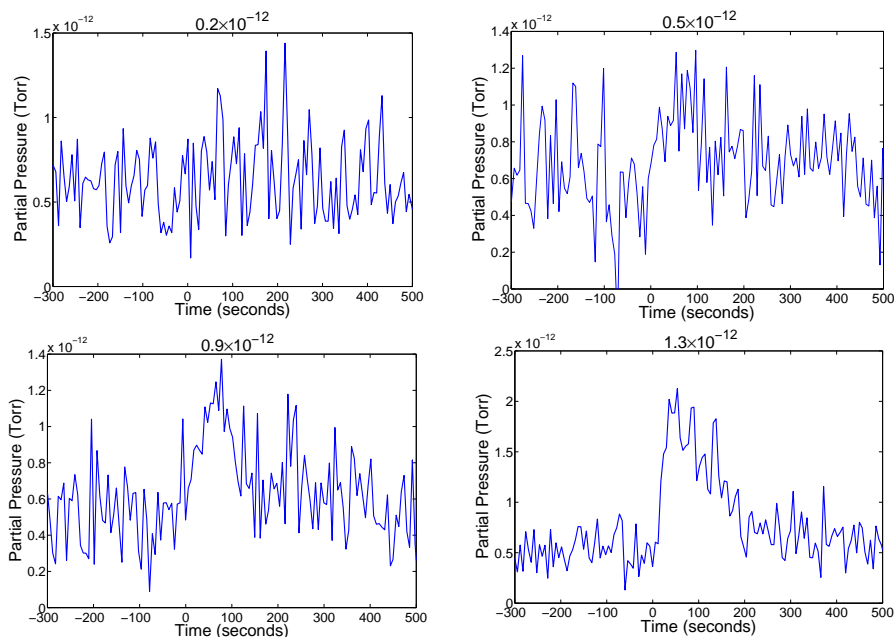


Figure 6: RGA response to the smallest concentrations of krypton. The krypton signals decay in time because the flow rate is decreasing due to the small amount of xenon available for these measurements. Upper left:  $0.2 \times 10^{-12}$  mol/mol. Upper right:  $0.5 \times 10^{-12}$  mol/mol. Lower left:  $0.9 \times 10^{-12}$  mol/mol. Lower right:  $1.3 \times 10^{-12}$  mol/mol.

it with small quantities of the 2.8 kg xenon supply, which contained  $99.5 \times 10^{-9}$  mol/mol of krypton after the experiments described in Section 4. For example, to achieve  $0.5 \times 10^{-12}$  mol/mol of krypton, we added 0.19 milligrams of our krypton-rich xenon supply to the 40 grams of de-kryptonated xenon. The sample was created by filling a volume of  $13.8 \pm 0.1$  cc with  $215.9 \pm 0.1$  Torr of xenon containing  $(99.5 \pm 4) \times 10^{-9}$  mol/mol of krypton and then volume sharing the gas with a  $1.5222 \pm 0.0005$  L volume to further reduce the pressure. With this simple method xenon samples could be prepared with krypton concentrations known to within 5% of the injection amount. The xenon was then analyzed by the cold trap mass spectrometry technique. Between each run we removed the extra krypton, and a new sample was mixed starting again with de-kryptonated xenon.

RGA partial pressure plots are shown in Figure 6 for xenon with 0.2, 0.5, 0.9, and  $1.3 \times 10^{-12}$  mol/mol of krypton. For the data shown in these plots we open the leak valve to its maximum setting at  $t = 0$  seconds. Since the total

$\rho(\text{Kr})$ ( $10^{-12}$ mol/mol)	Avg. $P_{\text{Kr}}$ ( $10^{-12}$ Torr)	Avg. Flow (SLPM)	Kr Fig. of Merit ( $10^{-12}$ Torr/SLPM)	Dev. from Fit (%)
$0.5 \pm 0.2$	0.406	1.32	$0.308 \pm 0.0154$	3.8
$0.9 \pm 0.2$	0.646	1.27	$0.507 \pm 0.0254$	5.1
$1.3 \pm 0.2$	1.15	1.28	$0.901 \pm 0.0450$	-12.4
$1.7 \pm 0.2$	1.37	1.28	$1.07 \pm 0.0528$	1.2
$5.1 \pm 0.3$	3.81	1.30	$2.93 \pm 0.147$	8.6
$17.1 \pm 0.9$	15.7	1.29	$12.2 \pm 0.608$	-13.7
$171.1 \pm 8.8$	127	1.27	$99.5 \pm 4.97$	6.9
* $1711 \pm 88$	1450	1.31	$1110 \pm 55.3$	-3.5
$1711 \pm 88$	1330	1.29	$1030 \pm 51.3$	4.1

Table 2: Results of krypton detection experiments with 40 grams of highly purified xenon. The various krypton concentrations were created by mixing with xenon containing  $99.5 \times 10^{-9}$  mol/mol krypton, except the sample labeled (\*), which was created by injecting 99.999% krypton from a krypton gas cylinder. For prepared samples of  $1.7 \times 10^{-12}$  mol/mol or less the uncertainty in the concentration is dominated by the minimum sensitivity to krypton in the highly purified xenon, which we take to be  $0.2 \times 10^{-12}$  mol/mol. For concentrations above  $1.7 \times 10^{-12}$  the uncertainty in the concentration is 5%, dominated by the uncertainty of the concentration of the krypton-rich xenon supply. The krypton figure of merit is the average partial pressure divided by the average flow rate. The last column shows the deviation from the linear fit shown in Figure 7.

amount of xenon available for these measurements is modest, the flow rate immediately peaks at 1.5 SLPM and then decreases during the measurement due to the decreasing pressure at the leak valve input. The resulting partial pressure plots follow this pattern, as shown in Figure 6.

Clear krypton signals are seen for concentrations of  $0.9 \times 10^{-12}$  mol/mol and larger, while the  $0.5 \times 10^{-12}$  mol/mol sample gives a marginal signal. No significant deviation from background is seen for the  $0.2 \times 10^{-12}$  mol/mol sample, which agrees with our expected sensitivity of  $0.25 \times 10^{-12}$  mol/mol (inferred by assuming partial pressure fluctuations of  $3 \times 10^{-13}$  Torr and a 1.5 SLPM flow rate.)

To quantify the krypton concentration, we calculate the average partial pressure in a 60 second window around its maximal value after subtracting the background level, and we divide by the average flow rate measured by the MKS mass flow meter. Since the same leak valve setting (fully open) was used in each dataset, the average flow rate varies by less than 2% in all datasets. As shown in Figure 7 and Table 2, the ratio of average pressure

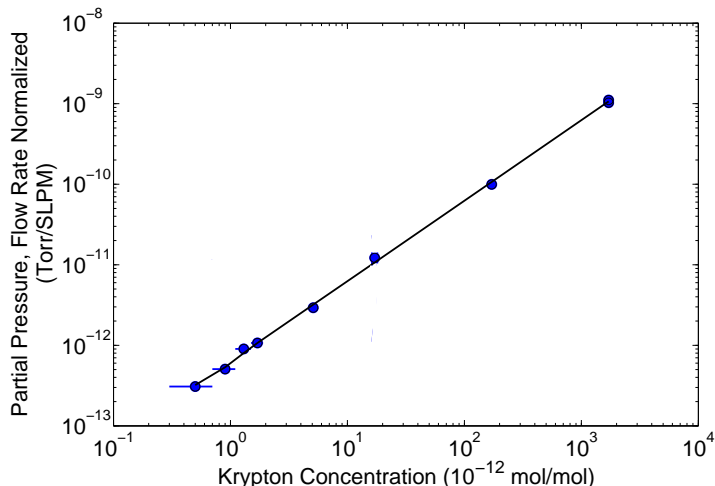


Figure 7: Krypton detection figure-of-merit as a function of true krypton concentration. The krypton partial pressure data (at 84 AMU) is averaged in a 60 second window around its peak value and then normalized to the average flow rate. The maximum deviation from a linear fit over three orders of magnitude is 13.7%. The solid line indicates the linear fit to the data.

to average flow rate is proportional to the true krypton concentration over four orders of magnitude. The linear dependence was expected as the peak partial pressure, for a fixed flow rate, should be proportional to the number of particles passing by the RGA per unit time. The largest deviation from the fitted line is 13.7%, and the dataset at  $0.5 \times 10^{-12}$  mol/mol deviates from the fitted line by only 4%. This indicates that the small krypton signal at  $0.5 \times 10^{-12}$  mol/mol is likely to be genuine, and demonstrates sensitivity to krypton at concentrations less than  $1 \times 10^{-12}$ . Previous methods have achieved sensitivities of about  $\sim 10^{-12}$  mol/mol [7, 8].

The linear dependence of the krypton figure-of-merit to concentration down to  $0.5 \times 10^{-12}$  mol/mol also demonstrates that the de-kryptonated xenon truly had an initial concentration less than  $0.5 \times 10^{-12}$  mol/mol. Had there been residual krypton in the xenon before the krypton injections, the data in Figure 7 would level off and not continue its linear decline at lower concentrations.

To confirm that the absolute krypton concentration of our experiments is not in error, we performed one final krypton injection from the krypton cylinder into our 40 grams of de-kryptonated xenon at a concentration of

$1.7 \times 10^{-9}$  mol/mol. This dataset gives a krypton figure of merit which agrees with the equivalent dataset produced by mixing to within 8%.

A second cross-check on our krypton concentration scale is provided by the EXO-200 double beta decay experiment. As reported in Ref. [13], EXO-200 has observed  $^{85}\text{Kr}$  in its natural (unenriched) xenon gas supply at a decay rate consistent with that inferred from our mass spectrometry technique, assuming that the  $^{85}\text{Kr}$  isotopic abundance is  $\sim 10^{-11}$ , as expected. This confirms our absolute scale to within a factor of two.

## 6. Conclusion

We have extended the xenon cold trap mass spectrometry technique to detect trace quantities of krypton in xenon gas. We find that krypton passes through the cold trap largely undisturbed, and that the resulting partial pressure is proportional to the true concentration after accounting for the flow rate. Using this method we have detected krypton concentrations as low as  $(0.5 \pm 0.2) \times 10^{-12}$  mol/mol  $^{nat}\text{Kr}/\text{Xe}$ .

Compared to the previously reported methods for krypton detection in xenon, our technique is rather simple and inexpensive, yet it achieves better sensitivity. It does not require any specialized equipment beyond an RGA, which most labs use routinely anyway.

We believe our sensitivity could be significantly improved by using faster flow rates, which could be achieved by using a larger sample of highly purified xenon. In principle we see no reason why an additional factor of ten improvement could not be achieved by using ten times the amount of xenon, which would make the technique useful for future WIMP dark matter experiments. In any case, the sensitivity demonstrated here will already be useful for krypton monitoring programs at existing detectors.

## 7. Acknowledgments

This work was supported by the National Science Foundation under award number PHY0810495.

## References

- [1] P. Collon, W. Kutschera, Z.-T. Lu, *Ann. Rev. Nucl. Part. Sci.* 54 (2004) 39–67.

- [2] D. McKinsey, et al., J. Phys. Conf. Ser. 203 (2010) 012026.
- [3] S. Fiorucci et al, AIP Conf. Proc 1200 (2010) 977.
- [4] K. Abe, J. Phys. Conf. Ser. 120 (2008) 042022.
- [5] E. Aprile, et al., Phys.Rev.Lett. 105 (2010) 131302.
- [6] E. Aprile, et al. [arXiv:1101.3866](https://arxiv.org/abs/1101.3866).
- [7] K. Abe, et al., Astropart. Phys. 31 (4) (2010) 290–296.
- [8] A. Bolozdynya, et al., Nucl. Instrum. Meth A 579 (1) (2007) 50–53.
- [9] D. N. McKinsey, C. Orzel, Nucl. Instrum. Meth. A545 (2005) 524–531.
- [10] D. Leonard, et al., Nucl. Instr. Meth. A 621 (1-3) (2010) 678 – 684.
- [11] A. Grutter, J. Shorrocks, Nature 204 (1964) 1084–1085.
- [12] A. Dobi, et al., Nucl. Instr. Meth. A 620 (2-3) (2010) 594 – 598.
- [13] S. Herrin, "Turn on of the EXO-200 detector", APS April Meeting 2011, Anaheim, CA, 2011.